Brain cine-MRI registration using MLSDO dynamic optimization algorithm

Julien Lepagnot, Amir Nakib, Hamouche Oulhadj and Patrick Siarry

Université Paris-Est Créteil (UPEC)
LISSI, E.A. 3956
61 avenue du Général de Gaulle, 94010 Créteil, France
siarry@u-pec.fr

Abstract

In this paper, we propose to use a dynamic optimization algorithm to assess the deformations of the wall of the third cerebral ventricle in the case of a brain cine-MRI. In this method, a segmentation process is applied to a 2D+t cine-MRI sequence to detect the contours of a region of interest (*i.e.* lamina terminalis). Then, the successive segmented contours are matched using a procedure of global alignment, followed by a registration process. This registration process consists in optimizing an objective function that can be considered as dynamic. Thus, a dynamic optimization algorithm, called MLSDO, is used in the registration process. The results obtained by MLSDO are compared to those of several well-known static optimization algorithms. This comparison shows the efficiency of MLSDO, and the relevance of using a dynamic optimization algorithm to solve this kind of problems.

1 Introduction

Image registration is the process of overlaying two or more images of the same scene taken at different times, from different viewpoints, and/or by different sensors. It is a critical step in all image analysis tasks in which the final information is gained from the combination of various data sources like, in image fusion or change detection.
It geometrically aligns two images: the source and the target images. It is done by determining a transformation that maps the target image to the source one. Thus, registering a sequence of images consists in determining, for each couple of successive images, the transformation that makes the first image of the couple match the following image.
If the successive images of the sequence are correlated, then we can make use of this correlation to accelerate the registration process. This can be done by using a *dynamic optimization* algorithm.

Recently, optimization in dynamic environments has attracted a growing interest, due to its practical relevance. Almost all real-world problems are time dependent or dynamic, *i.e.* their objective function changes over the time. For dynamic environments, the goal is not only to locate the global optimum, but also to track it as closely as possible over the time. Then, a dynamic optimization problem can be expressed as in (1), where $f(\vec{x}, t)$ is the objective function of a minimization problem, $h_j(\vec{x}, t)$ denotes the j^{th} equality constraint and $g_k(\vec{x}, t)$ denotes the k^{th} inequality constraint. All of these functions may change over the time (iterations), as indicated by the dependence on the time variable t.

$$\begin{array}{ll} \min & f(\vec{x}, t) \\ \text{s.t.} & h_j(\vec{x}, t) = 0 \text{ for } j = 1, 2, ..., u \\ & g_k(\vec{x}, t) \leq 0 \text{ for } k = 1, 2, ..., v \end{array} \quad (1)$$

In this paper, we focus on a dynamic optimization problem with time constant constraints. We propose to apply the *Multiple Local Search algorithm for Dynamic Optimization* (MLSDO) [5] to the registration of sequences of segmented images.

In the problem we deal with, each image contains segmented contours of the region of interest (*i.e.* lamina terminalis), extracted from a brain cine-MRI sequence of 20 images. This sequence corresponds to 80% of a R-R cardiac cycle [6], and the segmentation method used to generate these contours is

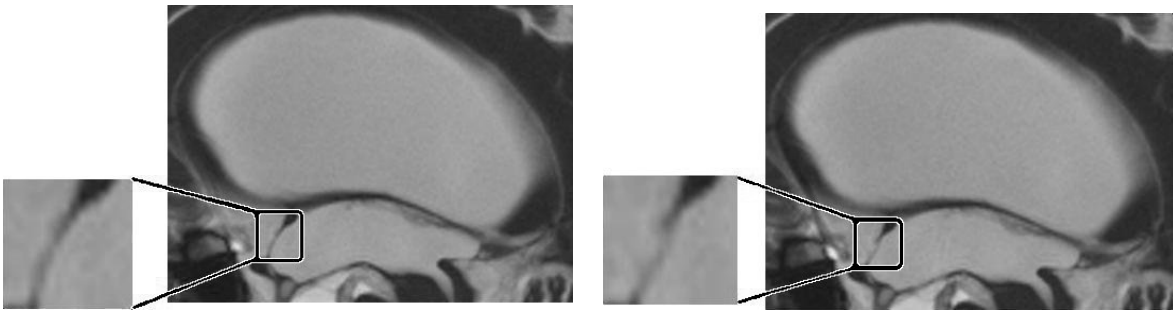

(a) (b)

Figure 1: Two images from a brain cine-MRI sequence: (a) first image of the sequence, (b) sixth image of the sequence.

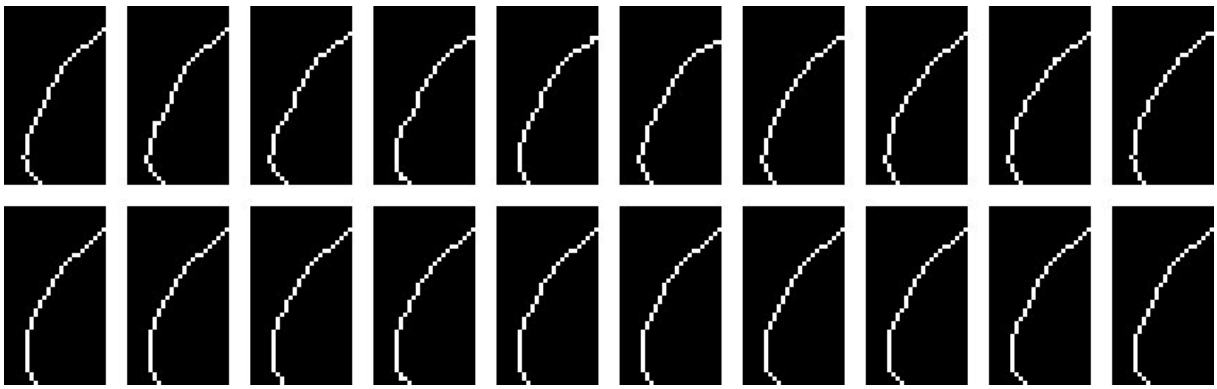

Figure 2: Sequence of segmented images.

described in [6]. An example of two images extracted from a brain cine-MRI sequence is presented in Figure 1. Hence, every segmented sequence is composed of 20 segmented cine-MRI. An example of segmented sequence is illustrated in Figure 2. The goal is to match the points of the contours in each couple of successive images of this sequence. The transformations that result from this matching operation can then be used to assess the deformation movements of the third cerebral ventricle.

Several papers are proposed in the literature about the analysis and quantification of cardiac movements, we can cite those recently published [1, 2, 8]. In our case, the single paper that deals with the problem at hand is [6], because of the recent appearance of the acquisition method. The main difference between the problem at hand and the cardiac problem lies in the amplitude of the movements of the ventricles. Indeed, the amplitude of the cardiac ventricle movements is higher than the amplitude of the cerebral ventricle movements. Then, a more accurate method is required in the cerebral case. In this paper, we propose a method inspired from [6] to assess the movements of a region of interest (ROI) from the wall of the third ventricle. The main contribution of the present work is to show the importance of the use of dynamic optimization algorithms for brain cine-MRI registration.

The rest of this paper is organized as follows. In section 2, the method proposed to register sequences of segmented contours is described. In section 3, the MLSDO algorithm and its use in the problem at hand are presented. In section 4, a comparison of the results obtained by MLSDO on this problem to the ones of several well-known static optimization algorithms is performed. This comparison shows the relevance of using MLSDO on this problem. Finally, a conclusion and the works under progress are given in section 5.

2 The registration method

A method inspired from [6] is proposed in this paper to register sequences of segmented contours. This operation is required in order to track the position of points belonging to the contours of the ROI over time. This operation is carried out in two steps: a matching step and a registration process.

2.1 The matching step

An example is presented in Figure 3 to illustrate this step. In Figure 3 (a) we present two synthetic contours to be aligned, the goal is to associate each point of the initial contours to one point of the second contours. We assume that each point of the first contours can be associated to at least one point of the second contours. Figure 3 (b) illustrates the goal of this procedure on real contours.

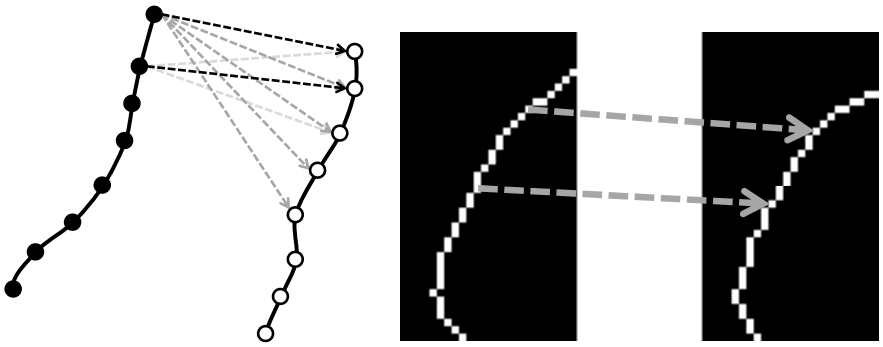

(a) (b)

Figure 3: Illustration of the matching procedure: (a) synthetic contours, (b) real contours of ROI (lamina terminalis) [6].

Let C_1 and C_2 be two curves consisting of L_1 and L_2 points, respectively, and corresponding to two successive contours of the sequence. Then, at the end of this alignment step, we get a set C_1' of sorted points of the contours C_2 that correspond to the contours C_1.

2.2 The registration process

Let the transpose of a matrix A be denoted by A^{T}.

In order to evaluate the pulsatile movements of the third cerebral ventricle in a way that it can be easily interpreted, a rigid transformation is used. We assume that a transformation T_Φ allows $C_2 = T_\Phi(C_1)$ and, for every point $(x_1 \;\; y_1)^{\mathrm{T}}$ of C_1, it is defined by:

$$\begin{pmatrix} x_2 \\ y_2 \end{pmatrix} = \begin{pmatrix} s_1.\cos\theta & -s_2.\sin\theta \\ s_1.\sin\theta & s_2.\cos\theta \end{pmatrix} \cdot \begin{pmatrix} x_1 \\ y_1 \end{pmatrix} + \begin{pmatrix} t_x \\ t_y \end{pmatrix} \tag{2}$$

Using homogeneous coordinates, (2) becomes:

$$\begin{pmatrix} x_2 \\ y_2 \\ 1 \end{pmatrix} = \begin{pmatrix} s_1.\cos\theta & -s_2.\sin\theta & t_x \\ s_1.\sin\theta & s_2.\cos\theta & t_y \\ 0 & 0 & 1 \end{pmatrix} . \begin{pmatrix} x_1 \\ y_1 \\ 1 \end{pmatrix} \tag{3}$$

The parameters s_1 and s_2 correspond to a homothetic transformation, θ corresponds to a rotation, t_x and t_y correspond to a translation operation. The set of parameters $\Phi = \{s_1, s_2, \theta, t_x, t_y\}$ is estimated through the minimization of the mean square error (MSE) computed on the set of points that will be paired. Then, the optimization criterion is given by:

$$MSE(\Phi) = \sum_{j=1}^{L_1} \frac{[C_1'(j) - T_\Phi(C_1(j))]^{\mathrm{T}} [C_1'(j) - T_\Phi(C_1(j))]}{L_1} \quad (4)$$

where $C_1'(j)$ and $C_1(j)$ denote the j^{th} point of C_1' and the j^{th} point of C_1, respectively.

The registration problem can be formulated as an optimization problem defined by:

$$\text{Min } MSE(\Phi) \quad (5)$$

Then, to avoid being trapped in a local optimum, we propose to use a metaheuristic on this problem.

3 The MLSDO algorithm

In this section, MLSDO and its use on the problem at hand are described. At first, the algorithm is presented. Then, the dynamic objective function proposed for the problem at hand is described. Afterwards, the parameter fitting of MLSDO is given to solve this problem.

3.1 Description of the algorithm

MLSDO has been developped in order to solve a wide range of dynamic optimization problems. It uses several local searches, each one performed in parallel with the others, to explore the search space, and to track the found optima over the changes in the objective function. These local searches consist in moving step-by-step in the search space, from a current solution to its best neighbor one, until a stopping criterion is satisfied, reaching thus a local optimum. Each local search is performed by an agent, and all the agents are coordinated by a dedicated module (the coordinator). Two types of agents exist in MLSDO: the exploring agents (to explore the search space in order to discover the local optima), and the tracking agents (to track the local optima over the changes in the objective function). The strategies used to coordinate these local search agents enable the fast convergence to well diversified optima, in order to quickly react to a change and find the global optimum. Furthermore, the local optima found during the optimization process are archived, to accelerate the detection of the global optimum after a change in the objective function. More details about this algorithm are in [5].

3.2 Cine-MRI registration as a dynamic optimization problem

The registration of a cine-MRI sequence can be seen as a dynamic optimization problem. Then, the dynamic objective function optimized by MLSDO changes according to the following rules:

- The criterion in (4) has to be minimized for each couple of contours, as we are in the case of a sequence, then the optimization criterion becomes:

$$MSE(\Phi(t), t) = \sum_{j=1}^{L_t} \frac{\left[C_t'(j) - T_{\Phi(t)}(C_t(j))\right]^{\mathrm{T}} \left[C_t'(j) - T_{\Phi(t)}(C_t(j))\right]}{L_t} \quad (6)$$

  where t is the index of the contours on which the transformation $T_{\Phi(t)}$ is applied, also equal to the index of the current couple of contours in the sequence. $\Phi(t)$, $C_t'(j)$, $C_t(j)$ and L_t are the same as Φ, C_1', C_1 and L_1 defined before, respectively, but here are dependent on the couple of contours.

- Then, the dynamic optimization problem is defined by:

$$\text{Min } MSE(\Phi(t), t) \quad (7)$$

- If the current best solution (transformation) found for the couple t cannot be improved anymore (according to a stagnation criterion), the next couple $(t + 1)$ is treated.
- The stagnation criterion of the registration of a couple of successive contours is satisfied if no significant improvement (higher than 1E-5) in the current best solution is observed during 200 successive evaluations of the objective function.
- Thus, the end of the registration of a couple of contours and the beginning of the registration of the next one constitute a change in the objective function.

3.3 Parameter fitting of MLSDO

Table 1 summarizes the six parameters of MLSDO that the user has to define. In this table, the values given are suitable for the problem at hand, and they were fixed experimentally. These values will be used to perform the experiments reported in the following section.

Name	Type	Interval	Value	Short description
r_l	real	$(0, r_e)$	1E-3	initial step size of tracking agents
δ_{ph}	real	$[0, \delta_{pl}]$	1E-7	highest precision parameter of the stopping criterion of the agents local searches
δ_{pl}	real	$[\delta_{ph}, +\infty]$	1E-5	lowest precision parameter of the stopping criterion of the agents local searches
n_a	integer	$[1, 10]$	1	maximum number of exploring agents
n_c	integer	$[0, 20]$	2	maximum number of tracking agents created after the detection of a change
r_e	real	$(0, 1]$	1E-1	exclusion radius of the agents, and initial step size of exploring agents

Table 1: MLSDO parameter setting for the problem at hand.

4 Experimental results and discussion

A comparison between the results obtained by MLSDO and those obtained by several well-known static optimization algorithms is presented in this section. These algorithms, and their parameter setting, empirically fitted to the problem at hand, are defined below (see references for more details on these algorithms and their parameter fitting):

- CMA-ES (*Covariance Matrix Adaptation Evolution Strategy*) [4] using the recommended parameter setting, except for the initial step size σ, set to $\sigma = 0.3$. The population size λ and the number of selected individuals μ are set to $\lambda = 8$ and $\mu = 4$;
- SPSO-07 (*Standard Particle Swarm Optimization* in its 2007 version) [3] using the recommended parameter setting, except for the number S of particles ($S = 6$) and for the parameter K used to generate the particles neighborhood ($K = 5$) ;
- DE (*Differential Evolution*) [7] using the "DE/target-to-best/1/bin" strategy, a number of parents equal to $NP = 12$, a weighting factor $F = 0.8$, and a crossover constant $CR = 0.9$.

As these algorithms are static, we have to consider the registration of each couple of successive contours as a new problem to optimize. Thus, these algorithms are restarted after the registration of each couple of contours, using the stagnation criterion defined in section 3.2. The results obtained using MLSDO, as a static optimization algorithm, are also given.

The parameters of the transformation model, found by each algorithm, are given in Tables 2-6, for the run having a median precision among 20 runs. In Table 7, the average number of evaluations among 20 runs of the algorithms are given. The average execution time of each algorithm, written in C, among 20

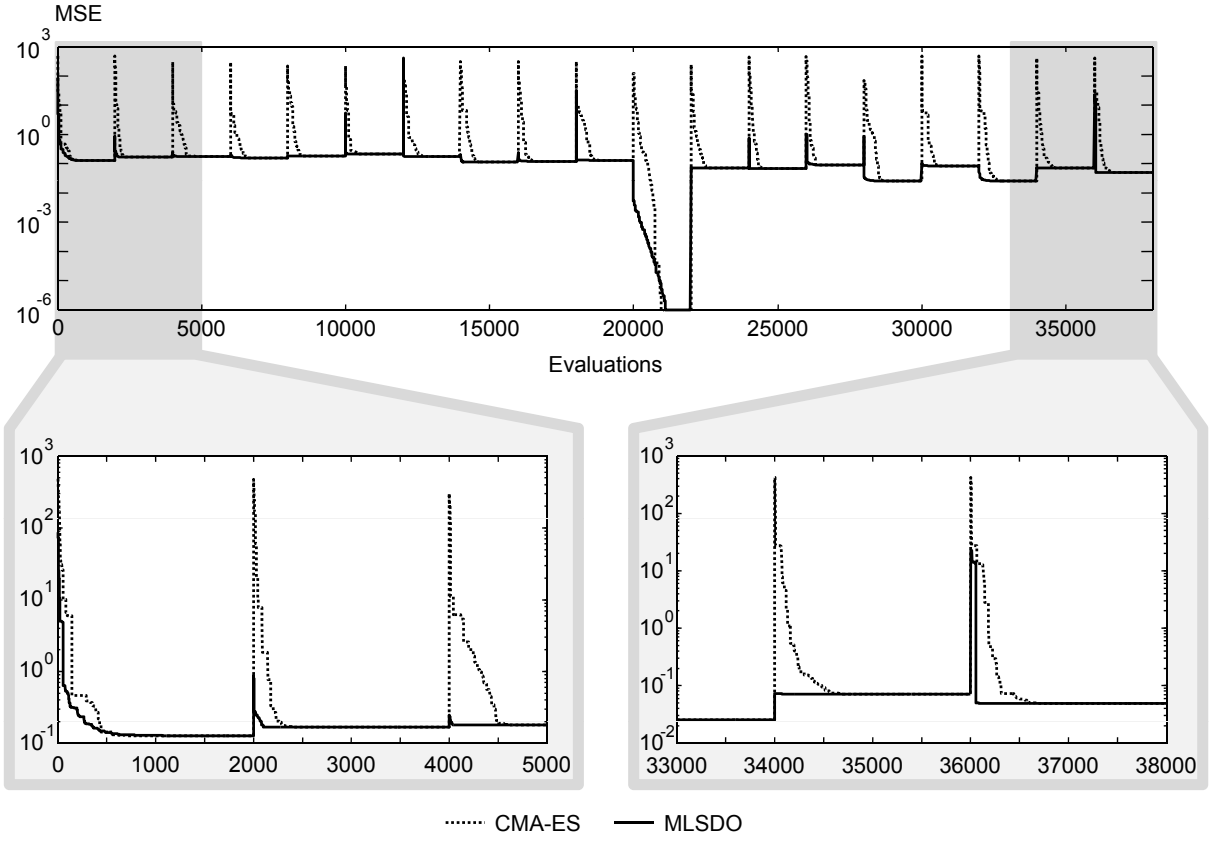

Figure 4: Convergence graph of MLSDO and CMA-ES on the problem at hand.

runs and using a 2.27 GHz Intel Core i5 processor, is also given. Additionally, the sum of the mean square errors (see equations (4) and (6)) of each registration of the sequence is given in this table, averaged on 20 runs of the algorithms. The convergence curve of MLSDO, and that of the best performing static optimization algorithm on the problem at hand, *i.e.* CMA-ES, are shown in Figure 4. In this figure, the number of evaluations per registration of a couple of contours is fixed to 2000, in order to enable the comparison of the convergence of the algorithms. For readability, a logarithmic scale is used on the ordinates.

As we can see in Tables 2-6, the transformations obtained by all algorithms are not significantly different: the values found for the parameters s_1, s_2, θ, t_x and t_y do not differ more than 5.9E-3, 1.8E-3, 3.0E-3, 3.7E-3 and 4.5E-3, respectively. Especially, the mean square error of the registration of a couple of contours does not differ more than 8.5E-5 between two algorithms. This level of precision is satisfying for the problem at hand. Then, the average sum of MSE given in Table 7 shows that the algorithms have a similar average precision.

However, we can see in Table 7 that the number of evaluations of the objective function performed by MLSDO, used as a dynamic optimization algorithm, is significantly lower than the ones of the static optimization algorithms. A Wilcoxon-Mann-Whitney statistical test has been applied on the numbers of evaluations performed by MLSDO and CMA-ES, the best ranked algorithms in terms of number of evaluations. This test confirms at a 99% confidence level that there is a significant difference between their performances. It can be seen also in Figure 4 that the convergence of MLSDO to an acceptable solution is faster than CMA-ES for the registration of all the couples of contours, except for the first one. MLSDO needs indeed to learn from the first registration in order to accelerate its convergence on the next ones. Thus, this comparison shows the efficiency of MLSDO and the significance of using a dynamic optimization algorithm on the problem at hand.

t	s_1	s_2	θ	t_x	t_y	$MSE(\Phi(t),t) \times 10^5$
1	1.021	0.999	-0.012	-0.005	0.147	12755.6
2	1.004	0.977	0.000	-0.021	0.336	16656.5
3	0.995	0.986	-0.004	0.042	0.213	17894.4
4	0.973	1.007	0.017	-0.023	0.123	15675.6
5	1.005	0.997	0.003	-0.096	0.116	18183.7
6	0.996	0.996	-0.005	-0.180	0.037	21043.2
7	1.017	0.993	-0.014	-0.264	0.005	17799.0
8	1.012	0.994	-0.011	-0.150	0.000	11328.8
9	0.961	1.000	0.000	-0.174	0.000	11961.9
10	0.988	0.997	-0.006	-0.132	0.000	13053.4
11	1.000	1.000	0.000	0.000	0.000	0.1
12	1.012	0.994	-0.012	-0.012	0.021	7118.1
13	1.016	0.993	-0.015	-0.039	-0.003	6891.8
14	0.976	1.007	0.015	-0.018	0.076	8927.5
15	1.004	1.000	-0.002	0.000	0.024	2535.8
16	1.033	0.987	-0.026	0.009	0.024	8197.4
17	1.006	0.999	-0.003	0.000	0.026	2550.3
18	1.012	0.998	-0.007	-0.002	0.076	7103.7
19	1.010	0.997	-0.006	-0.002	0.054	4922.5

Table 2: Transformations found by MLSDO, and their corresponding MSE, for the registration of each couple of contours.

t	s_1	s_2	θ	t_x	t_y	$MSE(\Phi(t),t) \times 10^5$
1	1.020	1.000	-0.011	-0.005	0.148	12754.4
2	1.002	0.977	0.001	-0.022	0.334	16652.8
3	0.993	0.986	-0.003	0.042	0.213	17891.9
4	0.972	1.008	0.018	-0.022	0.123	15674.1
5	1.008	0.996	0.002	-0.098	0.115	18179.6
6	0.999	0.995	-0.007	-0.181	0.036	21039.2
7	1.020	0.992	-0.016	-0.266	0.007	17795.1
8	1.010	0.995	-0.010	-0.150	0.002	11325.9
9	0.960	1.000	0.001	-0.173	0.000	11960.6
10	0.990	0.997	-0.007	-0.132	0.000	13051.7
11	1.000	1.000	0.000	0.000	0.000	0.0
12	1.014	0.994	-0.014	-0.012	0.023	7114.3
13	1.018	0.993	-0.016	-0.040	-0.002	6889.9
14	0.975	1.007	0.015	-0.019	0.077	8926.3
15	1.005	0.999	-0.003	0.000	0.024	2533.8
16	1.034	0.986	-0.026	0.008	0.025	8196.5
17	1.004	0.999	-0.002	-0.001	0.026	2548.4
18	1.013	0.998	-0.008	-0.002	0.075	7102.1
19	1.009	0.997	-0.005	-0.002	0.053	4922.0

Table 3: Transformations found by CMA-ES, and their corresponding MSE, for the registration of each couple of contours.

t	s_1	s_2	θ	t_x	t_y	$MSE(\Phi(t),t) \times 10^5$
1	1.021	0.999	-0.012	-0.005	0.149	12755.3
2	1.002	0.977	0.001	-0.022	0.334	16652.9
3	0.993	0.987	-0.003	0.042	0.213	17892.0
4	0.972	1.008	0.018	-0.021	0.125	15674.8
5	1.011	0.995	0.000	-0.100	0.120	18188.1
6	0.999	0.995	-0.006	-0.180	0.035	21039.3
7	1.020	0.992	-0.016	-0.268	0.006	17795.5
8	1.011	0.995	-0.010	-0.150	0.002	11326.3
9	0.961	1.000	0.001	-0.174	0.001	11960.8
10	0.990	0.997	-0.007	-0.131	-0.001	13051.7
11	0.998	1.000	0.001	-0.001	0.000	2.5
12	1.016	0.994	-0.014	-0.015	0.023	7117.0
13	1.018	0.993	-0.016	-0.040	-0.003	6889.9
14	0.974	1.007	0.015	-0.018	0.078	8926.6
15	1.006	0.999	-0.003	0.000	0.024	2533.9
16	1.034	0.986	-0.027	0.007	0.025	8196.7
17	1.004	0.999	-0.002	0.000	0.026	2548.7
18	1.013	0.998	-0.008	-0.002	0.075	7102.1
19	1.009	0.997	-0.005	-0.003	0.053	4922.4

Table 4: Transformations found by SPSO-07, and their corresponding MSE, for the registration of each couple of contours.

t	s_1	s_2	θ	t_x	t_y	$MSE(\Phi(t), t) \times 10^5$
1	1.020	1.000	-0.011	-0.004	0.148	12754.5
2	1.002	0.977	0.001	-0.021	0.334	16652.9
3	0.994	0.987	-0.003	0.041	0.212	17893.4
4	0.972	1.008	0.017	-0.022	0.122	15674.3
5	1.008	0.996	0.002	-0.097	0.116	18179.7
6	0.998	0.995	-0.006	-0.181	0.035	21039.5
7	1.020	0.992	-0.016	-0.267	0.006	17795.2
8	1.010	0.995	-0.010	-0.150	0.002	11325.9
9	0.960	1.000	0.001	-0.173	0.000	11961.1
10	0.990	0.997	-0.007	-0.131	0.000	13051.7
11	1.001	1.000	0.000	-0.001	0.000	0.4
12	1.015	0.994	-0.014	-0.012	0.023	7114.3
13	1.018	0.993	-0.016	-0.040	-0.003	6889.9
14	0.975	1.007	0.015	-0.019	0.077	8926.4
15	1.005	0.999	-0.003	-0.001	0.025	2533.9
16	1.034	0.986	-0.027	0.009	0.025	8196.5
17	1.004	0.999	-0.002	-0.001	0.026	2548.5
18	1.013	0.998	-0.007	-0.002	0.075	7102.2
19	1.009	0.997	-0.005	-0.002	0.053	4922.0

Table 5: Transformations found by DE, and their corresponding MSE, for the registration of each couple of contours.

t	s_1	s_2	θ	t_x	t_y	$MSE(\Phi(t), t) \times 10^5$
1	1.021	0.999	-0.012	-0.004	0.148	12755.6
2	0.998	0.978	0.003	-0.022	0.336	16661.0
3	0.995	0.986	-0.004	0.040	0.214	17893.5
4	0.973	1.007	0.017	-0.022	0.124	15675.7
5	1.010	0.995	0.001	-0.100	0.116	18181.9
6	1.000	0.995	-0.007	-0.182	0.037	21040.7
7	1.021	0.992	-0.017	-0.267	0.006	17797.2
8	1.012	0.994	-0.011	-0.149	0.004	11328.6
9	0.962	1.000	0.000	-0.174	0.000	11962.9
10	0.988	0.997	-0.006	-0.132	-0.001	13053.5
11	0.999	1.000	0.001	0.000	0.000	0.7
12	1.013	0.994	-0.013	-0.012	0.024	7115.2
13	1.017	0.993	-0.015	-0.039	-0.002	6890.6
14	0.976	1.007	0.015	-0.020	0.077	8927.3
15	1.007	0.999	-0.004	-0.001	0.026	2537.1
16	1.031	0.987	-0.026	0.008	0.027	8199.9
17	1.003	0.999	-0.002	-0.001	0.025	2549.4
18	1.012	0.999	-0.006	-0.003	0.076	7105.1
19	1.011	0.997	-0.006	-0.002	0.054	4923.2

Table 6: Transformations found by MLSDO used as a static optimization algorithm, and their corresponding MSE, for the registration of each couple of contours.

	Algorithm	Evaluations	Execution time (ms)	Cumulated MSE
Dynamic optimization	MLSDO	13841.80 ± 386.55	13.2 ± 5.7	2.05 ± 1.3E-4
Static optimization	CMA-ES	17651.65 ± 288.10	5029.5 ± 212.8	2.05 ± 1.6E-2
	SPSO-07	19611.70 ± 994.13	49.8 ± 22.5	2.05 ± 2.7E-2
	DE	21749.60 ± 869.46	56.4 ± 23.4	2.05 ± 2.8E-5
	MLSDO	28891.15 ± 908.88	29.8 ± 20.3	2.05 ± 1.8E-4

Table 7: Average number of evaluations and execution time to register all couples of contours, and average sum of MSE, obtained by each algorithm.

5 Conclusion

In this paper, a registration process based on a dynamic optimization algorithm, called MLSDO, is proposed to register quickly all the segmented images of a cine-MRI sequence. It takes profit from the effectiveness of the dynamic optimization paradigm. As MLSDO is not specifically designed for the problem at hand, but to solve a wide range of problems, the method proposed in this paper can be also applied to other kinds of sequences. The process is sequentially applied on all the 2D segmented images. The entire procedure is fully automated and provides an accurate assessment of the ROI deformation throughout the entire cardiac cycle. Our work under progress consists in an open source software encapsuling the proposed method. We are also working on the use of an elastic deformation model in order to improve the precision of the registration process of the contours.

References

[1] M. J. Budoff, N. Ahmadi, G. Sarraf, Y. Gao, D. Chow, F. Flores, and S. S. Mao. Determination of left ventricular mass on cardiac computed tomographic angiography. *Academic Radiology*, 16(6):726–732, 2009.

[2] Y. Chenoune, E. Deléchelle, E. Petit, T. Goissen, J. Garot, and A. Rahmouni. Segmentation of cardiac cine-MR images and myocardial deformation assessment using level set methods. *Computerized Medical Imaging and Graphics*, 29(8):607–616, 2005.

[3] M. Clerc *et al.* The *Particle Swarm Central* website. http://www.particleswarm.info.

[4] N. Hansen and A. Ostermeier. Completely derandomized self-adaptation in evolution strategies. *Evolutionary Computation*, 9(2):159–195, 2001.

[5] J. Lepagnot, A. Nakib, H. Oulhadj, and P. Siarry. A multiple local search algorithm for continuous dynamic optimization. Under submission.

[6] A. Nakib, F. Aiboud, J. Hodel, P. Siarry, and P. Decq. Third brain ventricle deformation analysis using fractional differentiation and evolution strategy in brain cine-MRI. In *Medical Imaging 2010: Image Processing*, volume 7623, pages 76232I–1–76232I–10, San Diego, California, USA, 2010. SPIE.

[7] K. Price, R. Storn, and J. Lampinen. *Differential Evolution - A Practical Approach to Global Optimization*. Springer, 2005.

[8] H. Sundar, H. Litt, and D. Shen. Estimating myocardial motion by 4D image warping. *Pattern Recognition*, 42(11):2514–2526, 2009.